International Journal of Computer Information Systems and Industrial Management Applications
ISSN 2150-7988 Volume 18(22s) 2026 pp. 228-253
https://doi.org/10.70917/ijcisim-2026-5429
Article

Numerical optimization of VRM Cyclone Geometry for Enhanced Energy efficiency

Rajpal Singh Shekhawat[1], Pushpendra Kushwaha[2], Dr. Madhu Agarwal[3*]

[1]Research scholar, Department of Chemical Engineering, Malaviya National Institute of Technology, Jaipur – 302017, Rajasthan, India
Email Id: 2020rch9028@mnit.ac.in
[2]Research scholar, Department of Chemical Engineering, Malaviya National Institute of Technology, Jaipur-302017, Rajasthan, India
Email Id: 2020rch9551@mnit.ac.in
[3]Professor, Department of Chemical Engineering, Malaviya National Institute of Technology, Jaipur- 302017, Rajasthan, India
*Corresponding Email Id: magarwal.chem@mnit.ac.in
ORCID ID: 0000-0003-2330-195X

Abstract: The cement industry, which is a highly energy-intensive industry as well as a rapidly growing sector, is grappling with various challenges like increasing power, fuel, and raw material costs which are leading to diminishing profit margins. In order to survive and sustain and expand profit margin, plant went for capacity enhancement by increasing the feed of the Vertical roller mill. However, it led to an increased pressure drop of 200-210 mmWG across the cyclone against the typical value of 120-130 mmWG. This paper unveils the deliberation of reduction in pressure drop with the help of Computational Fluid Dynamics (CFD) across the cyclone to reduce power consumption of raw mill fan. CFD was employed to understand the flow patterns across the cyclone separator. Non-uniform flow of flue gas at the inlet of the cyclone was observed. To make the uniform flow pattern, guide plates were installed and the cyclone's inlet area was enlarged, and the modification resulted in the pressure drop reduction of 40 mmWG and savings of 0.18 kWh/t material in the raw mill fan.
Keywords: Pressure drop; CFD analysis; Cyclone separator; Raw mill fan; Gas flow

1. INTRODUCTION

Capacity enhancement and technology upgradation have been incessant in the cement industries catering to the precipitous rise in demand for building materials due to rapid urbanization and population explosion. However, sometimes, an increase in production comes with increases in power consumption, which ultimately leads to increased indirect emissions. The cement industry is one of the major energy intensive industries which is responsible for 7% of anthropogenic CO2 emissions. Raw meal and clinker grinding power are major contributors to the specific power consumption of the cement plant. VRM is one of the commonly used grinding mills in cement plants having higher energy efficiency than classical ball mills. The grinding circuits are often equipped with cyclones which separate dust from gas or for product recovery. They are widely used because of their geometrical simplicity, relative economy in power usage adaptability to extremely harsh conditions and flexibility. The function of the cyclones is based on pressure differences, centrifugal and centripetal forces formed by the vortex of the medium. The inlet velocity of the stream is the most important factor affecting the pressure drop, in turn directly affecting efficiency [1,2]. The cyclone is a relatively simple instrument with no moving parts. However, the flow inside a gas cyclone is quite complicated with strong gas-solids interaction and a huge number of multi-sized particles [3]. Due to the hydrodynamic complexity of cyclones, no exact mathematical model for cyclones has been offered yet. Here, CFD serves as a tool for numerical solutions [4,5]. This paper unveils the deliberation of reduction in pressure drop across the cyclone with the help of computational fluid dynamics (CFD) to reduce power consumption of raw mill fan.

In the initial ages, analytical fluid dynamics (AFD) and experimental fluid dynamics (EFD) were used in the problem associated with fluid flow. But later, Computational fluid dynamics (CFD) became an efficient and economical approach to understand fluid dynamics, providing an efficient way to evaluate how the dynamics are affected by changes in operating conditions and geometric shapes. CFD is a branch of fluid mechanics that uses numerical analysis and data structures to analyze and solve problems that involve fluid flows [6–8]. The prediction is quantitative in which the conservation of mass, energy, and momentum of fluid takes place. CFD is used for the simulation of fluids engineering systems that use modeling (mathematical physical problem formulation) and numerical methods (discretization methods, solvers, numerical parameters, and grid generations). CFD is applied to a wide range of research and engineering problems in many fields of study and industries [9]. Pre-processing, solving the problem, and post-processing are the three main phases in the CFD. Some of the studies investigated cyclone optimization using CFD applications. Katare et al. designed a hydro cyclone that was used for filtration, i.e., for cleaning machines, therefore; to examine its performance and its efficiency is calculated using CFD [10]. The simulation results showed that pressure increased from the center to the wall. In this chain, maximum and minimum velocity were determined to be 12.5 m/s and 0.55 m/s respectively. Chu et al. adopted discrete element method (DEM) and CFD models to study the gas-solid flow in a gas cyclone [11]. On increasing solid ratio, less turns traveled by solids (apex region) and total mass did not increase linearly. During solid loading gas pressure drop initially increased and after that, it decreases to attain a stable value. The total and average particle-particle interaction enhanced with an increasing solid ratio. Mirzaei et al. used a hybrid multiphase model (Dense discrete phase model, DDPM) for performing simulation corresponding to the cyclone preheaters operating at elevated solid loadings [12]. The model results were validated through the industrial cyclone preheater, which had 1.6 m diameter. The investigation revealed that pressure drops, overall heat transfer rate, and flow pattern due to changes in operating conditions were accurately predicted by the adopted model. Elsayed et al. used Muschelknautz modelling method for optimizing the cyclone's geometrical ratios [13]. CFD simulation aided with the Reynolds stress model was used during entire investigation to achieve the minimum pressure drop by using a new set of geometrical ratios. Numerical simulation and Stairmand design authenticate the superior performance of the newly developed design. Chu et al. developed a coarse grained combined Discrete element method (DEM) and CFD models for numerical study of gas-solid flow inside the gas cyclone, in which particle size distribution ranged from 1-200 μm [14]. Their investigation by CFD-DEM model predicted the separation efficiency for the fine particles. Thus, very few studies are available focusing on pressure drop optimization for raw mill cyclones of cement plants.

This paper unveils the deliberation of reduction in pressure drop across the cyclone without compromising the collection efficiency with the help of Computational Fluid Dynamics (CFD) to reduce power consumption of raw mill fan.

2. Background

Vertical roller mills equipped with cyclones are commonly used in cement plants in raw material grinding circuits. Cyclone acts as a separation equipment separating fine product from the gas stream. VRM for a cement plant in this case was originally designed for grinding limestone with a capacity of 250 TPH. However, feed surged to 325 TPH, driven by enhancements in clinker production and raw meal utilization for clinker manufacturing. However, this heightened capacity led to an elevated velocity at the cyclone inlet, currently measured at 22 m/s compared to the normal value of 15 m/s. Consequently, there was a notable rise in pressure drop across the cyclone, reaching levels between 195-205 mmWG against the normal value of 120-130 mmWG leading to increased fan power consumption impacting overall efficiency. The probable reason for this high-pressure drop could be attributed to turbulence and dead zones in the flow, along with pressure loss due to internal friction caused by fluid viscosity. Investing in new low-pressure drop cyclones presented challenges due to significant investment requirements and space constraints. Subsequently, Computational Fluid Dynamics (CFD) was applied across cyclones to reduce the pressure drop to normal operating range without compromising the current collection efficiency of the cyclone.

Simulation procedure

Initially, modelling is done for the geometry domain, and the modelling of flow mainly includes geometry and domain, coordinates, governing equations, flow conditions, initial and boundary conditions, and selection of models for different applications. The modelling geometry is done with the help of CAD software packages. The geometry and flow domain are modeled in such a manner as to provide input for the grid generation. Next step is to assign the initial and boundary conditions which is used to define a problem, and at the same time it exhibits the primary importance in CFD. It is because the applicability of numerical methods and the resultant quality of computations can critically be decided on how those are numerically treated. Basically, the problem starts with an initial condition and uses an iteration method to reach the final condition.

Generation of the grid is the next crucial step, and this step in CFD refers to a set of techniques for defining a numerical mesh throughout the system to be simulated [15] . In this analysis, meshing or grid generation is done by ICEM CFD 15.00 technique. The ICEM CFD is the powerful tool for mesh preparation [16] . The steps involved in the grid generation are geometry creation in solid works, geometry file is imported in .txt file to ICEM CFD, domain creation, association of different edges and vertices related to geometry's curve, assigning of number of nodes for mesh generation, and the last step is to check the quality of the mesh. The next step is to establish the simulation strategy; the simulation is carried out by Ansys software. The simulation associate with the process requires several inputs of the files and these files are grid file, initial solution file, input data file, and auxiliary files (i.e. multi-processor, local boundary conditions, chemistry and so on). Input parameters are established after simulation strategy and in this scenario the pre-processing part of a CFD problem is the first step before starting to process the problem. CFD codes generally require an input data file that can be created for listing the value of the input parameter with the desired strategy and further the grid file containing the grid and boundary condition information. Further, simulation is performed by adopting marching methods to determine iterative convergence. Next step was to monitor the CFD simulation through the various available packages such as FAST, Field view, Insight, Tec Plot, CFPOST. At last, post processing is required that includes analysis and visualization of the problems. Calculation of derived variables, calculation of integral parameters, and visualization of contour and surface plots are the three major sections of the post processing processes.

Cyclone geometry

A cyclone separator is a tool widely used for separating particles because of its simple design and low cost of construction and operation [17]. When the mixed phase enters the cyclone separator, the phase will move around its surface and form the outer vortex region (quasi-free vortex). Consequently, the solid phase will separate from the cyclone and collect at the bottom. In contrast, the gas phase will exit through the outlet and form the inner vortex (quasi-forced vortex) [18] . There exists the tangential flow of gas inside the cylindrical section of the cyclone and double vortex flow process inside the cyclone separator that makes this process very complicated [19] . In the present investigation, the pressure drop indicates the difference in pressure at the inlet and the outlet surfaces. Pressure drop is proportional to the energy that a cyclone would require to operate. Higher pressure drops results in large irreversible losses, and so, higher energy is needed to make the fluid flow through the cyclone volume, and vice-versa. Turbulence and dead zone in the flow might be the probable reason for the high pressure drop. Pressure loss due to internal friction arises because the fluid viscosity was an additional pressure loss created by the turbulence. The geometry and the dimensions of the cyclone separator are shown in Fig. 1, 2, and 3.

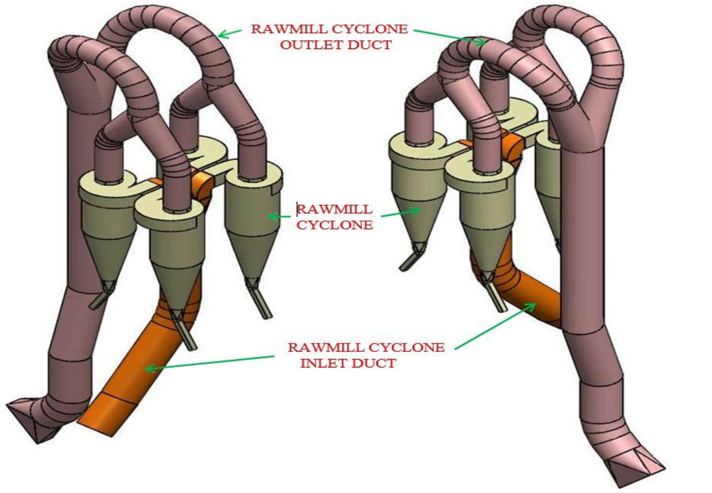

Figure 1. The Isometric view of Raw Mill Duct.

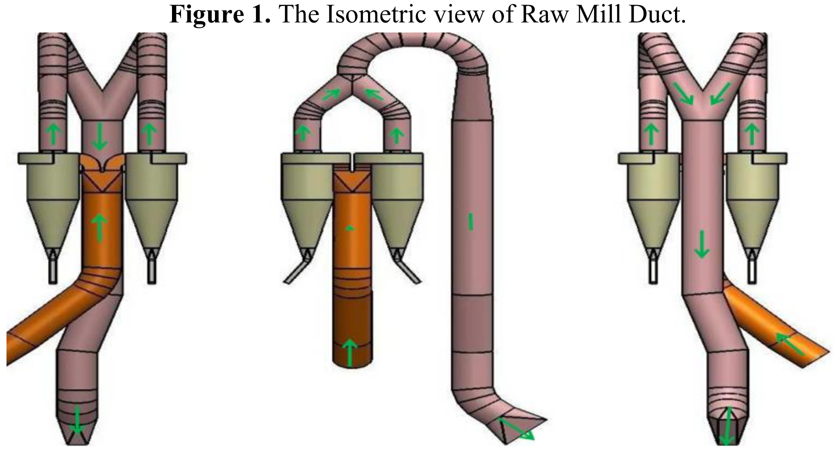

Figure 2. The flow direction details of Raw mill duct.

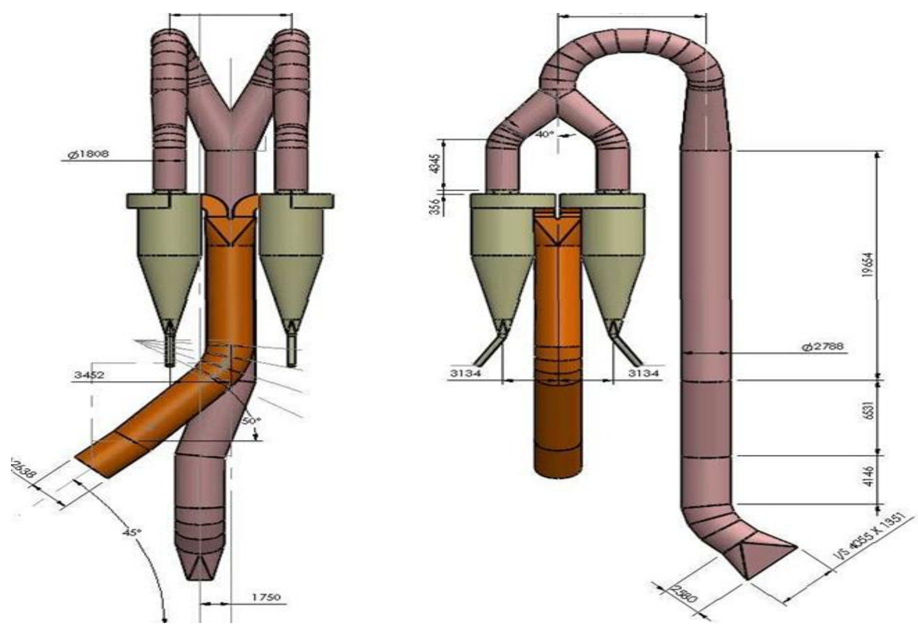

Figure 3. Dimensional details of Raw Mill Duct.

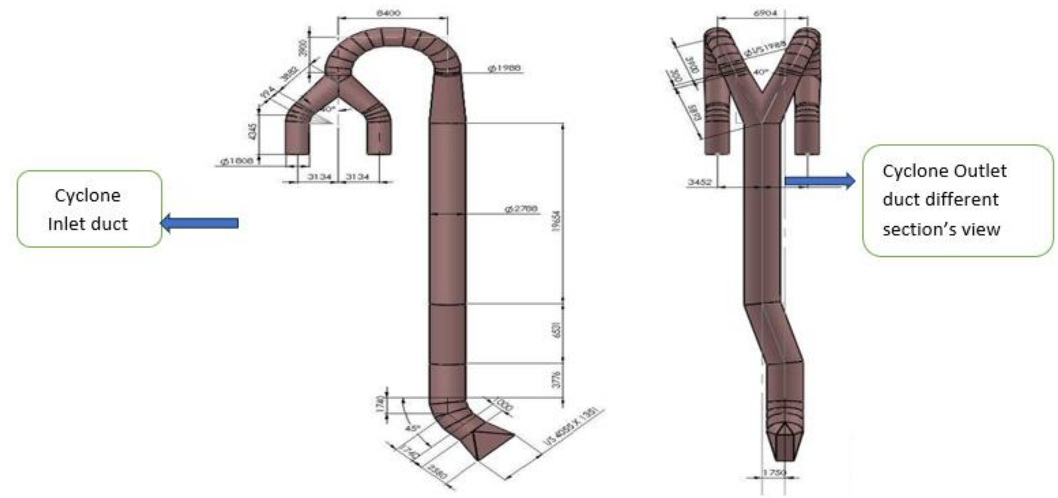

3. Figure 4. Dimensional details of Raw Mill Duct.

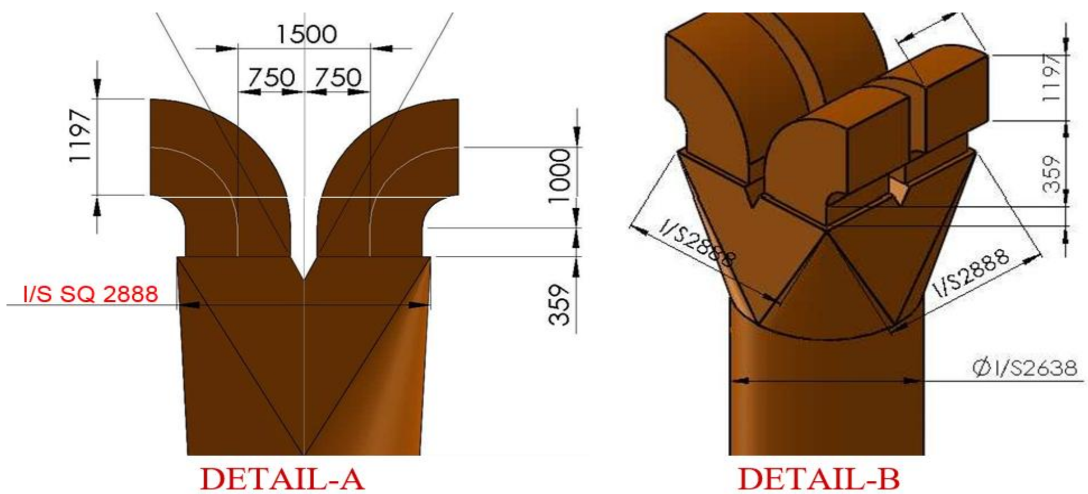

Figure 5. Dimensional details of Raw Mill Duct.

Mesh Generation using ICEM CFD

To perform CFD analysis, the model must be split into small elements. The prediction of the results is highly dependent on grids. We used high quality structured mesh for the CFD analysis [20]. Grid generation is prepared using commercial CFD code Ansys-ICEM CFD. This is a powerful tool for Meshing. The Mesh control is high, and Hexahedral type of meshing is possible with this tool. In the current model High Quality Hexahedral Structured mesh is prepared for Grid Preparation [21].

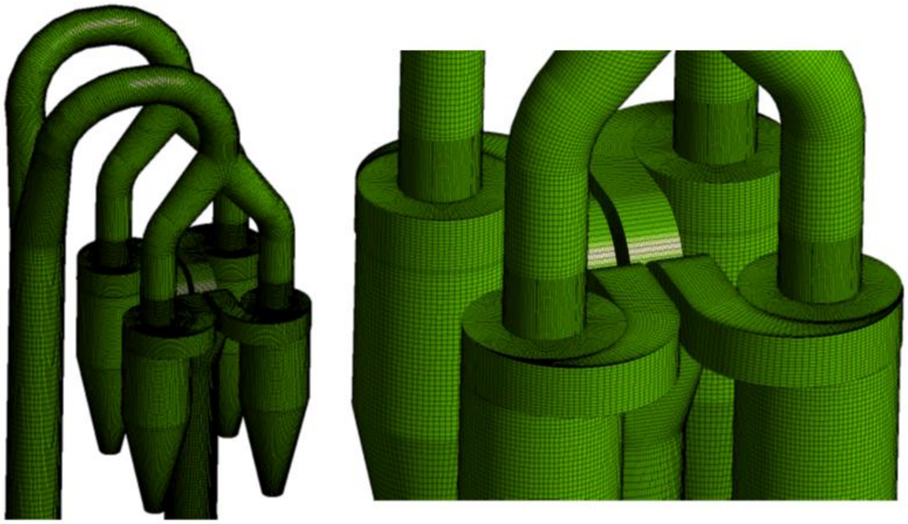

4. Figure 6. Details of Mesh created using ICEM CFD.

By solving Reynolds-averaged Navier–Stokes equations (RANS equations) for many different boundary conditions, using ANSYS CFX & Fluent to visualize the flow pattern in every point called simulation in CFD (by simulation we can see reactions, turbulence and heat transfer, mass transfer and velocities in the design) [22] . The Simulation is done using Commercial CFD Solver Ansys CFX. For Analysis of turbomachines, Ansys-CFX is the best tool.

Governing equations used in study

Reynolds stress model (RSM)

The Reynolds stress model (RSM) is the most explored form of the CFD Model. It works on principle that the isotropic eddy-viscosity hypothesis is abandoned, and the RSM closes the Reynolds-averaged Navier-Stokes equations by solving transport equations for the Reynolds stresses, together with an equation for the dissipation rate [23]. The RSM provides effects of streamline curvature, swirl, rotation, and rapid changes in strain rate in a more rigorous manner than one-equation and two-equation models; it has greater potential to give accurate predictions for complex flows. The modeling of the pressure-strain and dissipation-rate terms is particularly challenging and often considered to be responsible for compromising the accuracy of RSM predictions [24].

The RSM is a must when the flow features of interest are the result of anisotropy in the Reynolds stresses. Examples are cyclone flows, highly swirling flows in combustors, rotating flow passages, and the stress-induced secondary flows in ducts.

The Reynolds Stress Equation Model is as follows:

Three-dimensional flow occurs in a cyclone. Therefore, CFD simulation is realized using the conservation equation: mass, momentum, and energy in the incompressible flow at Equations [25].

$\frac{\partial \rho}{\partial x} + \frac{\partial}{\partial x}(\rho u_i) = 0$ (continuity/mass eq.) (1)

$\frac{\partial}{\partial x}(\rho u_i) + \frac{\partial}{\partial x_j} = -\frac{\partial p}{\partial x_i} + \frac{\partial}{\partial x_j}\left[\mu\left(\frac{\partial u_i'}{\partial x_j} + \frac{\partial u_j'}{\partial x_i}\right)\right] + \frac{\partial}{\partial x_j}\left(-\rho \underline{u_i' u_j'}\right)$ (momentum eq.) (2)

$\frac{\partial}{\partial x_j}\left(\rho C_p u_i T\right) = \frac{\partial}{\partial x_i}\left(k\frac{\partial T}{\partial x_i} - \rho C_p \underline{vt}\right)$ (energy eq.) (3)

$u_i = \underline{u_i} + u_i'$ (actual velocity) (4)

Where ρ is gas density, x_i is the position, the pressure (P), the fluctuating velocity component (u_i'), the mean velocity ($\underline{u_i}$), the viscosity (μ), and the Reynold stress tensor $\left(-\rho\underline{u_i' u_j'}\right)$. For example, Eq. (3) shows that T and t are fluctuating temperature and time average components, respectively. The transport RSM was used to express below.

The exact transport equations for the transport of the Reynolds stresses, $\rho\underline{u_i' u_j'}$, may be written as follows:

$$\underbrace{\frac{\partial}{\partial x}\left(\rho\underline{u_i'u_j'}\right)}_{Local\ Time\ Derivative} + \underbrace{\frac{\partial}{\partial x_k}\left(\rho u_k\underline{u_i'u_j'}\right)}_{C_{ij}\equiv Convection}$$
$$= \underbrace{\frac{\partial}{\partial x_k}\left[\left(\rho\underline{u_i'u_j'u_k'}\right) + \underline{p'\left(\delta_{kj}u_i' + \delta_{ik}u_j'\right)}\right]}_{D_{Tij}\equiv Turbulent\ Diffusion}$$
$$+ \underbrace{\frac{\partial}{\partial x_k}\left[\mu\frac{\partial}{\partial x_k}\left(\underline{u_i'u_j'}\right)\right]}_{D_{Lij}\equiv Molecular\ Diffusion} \underbrace{- \rho\left(\underline{u_i'u_k'}\frac{\partial u_j}{\partial x_k} + \underline{u_j'u_k'}\frac{\partial u_i}{\partial x_k}\right)}_{P_{ij}\equiv Stress\ Production}$$
$$\underbrace{- \rho\beta\left(g_i\underline{u_j'\theta} + g_j\underline{u_i'\theta}\right)}_{G_{ij}\equiv Buoyancy\ Production}$$
$$+ \underbrace{\underline{p'\left(\frac{\partial u_i}{\partial x_j} + \frac{\partial u_j}{\partial x_i}\right)}}_{\varphi_{ij}\equiv Pressure\ Strain} - \underbrace{2\mu\underline{\frac{\partial u_i'}{\partial x_k}\frac{\partial u_j'}{\partial x_k}}}_{\varepsilon_{ij}\equiv Dissipation}$$
$$\underbrace{- 2\rho\Omega_k\left(\underline{u_j'u_m'}\varepsilon_{ikm} + \underline{u_i'u_m'}\varepsilon_{jkm}\right)}_{F_{ij}\equiv Production\ by\ System\ Rotation}$$
$$+ \underbrace{S_{user}}_{User\ Defined\ Source\ Term}$$

Where,

δ= Internal Strain due to fluid motion

g = Gravitational constant

β= Volume Expansion Coefficient

θ= Temperature gradient

Ω= Vorticity

i, j, k= Unit Vectors along x, y, z axis

The Reynolds stress model (RSM) is the most explored form of RANS turbulence model. It works on principle that it the isotropic eddy-viscosity hypothesis is abandoned and the RSM closes the Reynolds-averaged Navier-Stokes equations by solving transport equations for the Reynolds stresses, together with an equation for the dissipation rate. The RSM provides effects of streamline curvature, swirl, rotation, and rapid changes in strain rate in a more rigorous manner than one-equation and two-equation models; it has greater potential to give accurate predictions for complex flows. The modeling of the pressure-strain and dissipation-rate terms is particularly challenging and often considered responsible for compromising the accuracy of RSM predictions.

ε-based Reynolds stress models

1. linear pressure-strain model
2. quadratic pressure-strain model

ω-based Reynolds stress models

1. stress-omega model
2. stress-BSL model

The RSM is a must when the flow features of interest are the result of anisotropy in the Reynolds stresses. The examples are like cyclone flows, highly swirling flows in combustors, rotating flow passages, and the stress-induced secondary flows in ducts

Linear Pressure-Strain Model

In this case, compressible fluids with high pressure and kinetic energy are examined. Due to the presence of high flow rate and energy, the momentum equation has an additional term which needs to solve the deformation due to motion at high pressure [26]. This can be expressed by linear pressure strain equation and can be considered as add-on for Reynolds stress equation.

By default, in Ansys Fluent, the pressure-strain term, φ_{ij} , in Equation above, is modeled according to the proposals by Gibson and Launder.

The classical approach to modeling φ_{ij} uses the following decomposition:

$$\varphi_{ij} = \varphi_{ij,1} + \varphi_{ij,2} + \varphi_{ij,w}$$

where $\varphi_{ij,1}$ is the slow pressure-strain term, also known as the return-to-isotropy term, $\varphi_{ij,2}$ is called the rapid pressure-strain term, and $\varphi_{ij,w}$ is the wall-reflection term.

The slow pressure-strain term, $\varphi_{ij,1}$ is modeled as

$$\varphi_{ij,1} \equiv -C_1 \rho \frac{\varepsilon}{k}\left[\underline{u_i' u_j'} - \frac{2}{3}\delta_{kj} k\right]$$

Where $C_1 = 1.8$ (its Constant) , ε= Linear strain due to motion, k= Bulk modulus

The rapid pressure-strain term $\varphi_{ij,2}$ is modeled as

$$\varphi_{ij,2} \equiv -C_2\left[\left(P_{ij} + F_{ij} + \frac{5}{6}G_{ij} - C_{ij}\right) - \frac{2}{3}\delta_{ij}\left(P + \frac{5}{6}G - C\right)\right]$$

Where, $C_2 = 0.60$, P_{ij}, F_{ij}, G_{ij} and C_{ij} are defined as in equation above and,

$P = \frac{1}{2}P_{kk}$ $G = \frac{1}{2}G_{kk}$ and $C = \frac{1}{2}C_{kk}$

The wall-reflection term, $\varphi_{ij,w}$ is responsible for the redistribution of normal stresses near the wall.

It tends to damp the normal stress perpendicular to the wall, while enhancing the stresses parallel

to the wall. This term is modeled as,

$$\varphi_{ij,w} \equiv C_1' \frac{\varepsilon}{k}\left(\underline{u_k' u_m'} n_k n_m \delta_{ij} - \frac{3}{2}\underline{u_i' u_k'} n_j n_k - \frac{3}{2}\underline{u_i' u_k'} n_i n_k\right)\frac{C_l K^{\frac{3}{2}}}{\varepsilon d} + C_2'\left(\varphi_{km,2} n_k n_m \delta_{ij} - \frac{3}{2}\varphi_{ik,2} n_j n_k - \frac{3}{2}\varphi_{jk,2} n_i n_k\right)\frac{C_l K^{\frac{3}{2}}}{\varepsilon d}$$

Where, $C_1'$and C_2' are constants for approximation of equations and considered to be constants $C_1' = 0.5$, $C_2' = 0.3$, n_k is the X_k component of the unit normal to the wall, d is the normal distance to the wall, and $C_l = \frac{C_\mu^{\frac{3}{4}}}{k}$ where $C_\mu = 0.09$ and K is the von Kármán constant (= 0.4187). $\varphi_{ij,w}$ is included by default in the Reynolds stress model.

Software Package Ansys-Fluent is used to solve these equations. The fluent is the most suitable software for core capturing.

The residual convergence criteria are set at 10-4 for continuity and 10-3 for X-Velocity, Y- Velocity, Z-Velocity, UV, VW, and WU stresses [27].

Boundary Conditions

The boundary condition of the CFD is from VRM outlet duct to Raw mill fan inlet duct and it is further divided into three parts-

1. Raw Mill outlet to Cyclone inlet
2. Cyclone inlet to cyclone outlet
3. Cyclone outlet to Raw mill fan inlet.

However, the main objective of the study is to see in detail how pressure drop across cyclone can be reduced

Following process parameters used to conduct CFD simulation -

Flow Rate at fan inlet: 4,69,194 m3/hr

Pressure at VRM fan inlet: -1150 mmWC

Temperature at fan inlet: 87 °C

Boundary condition: Vertical Mill Outlet duct to Mill fan inlet

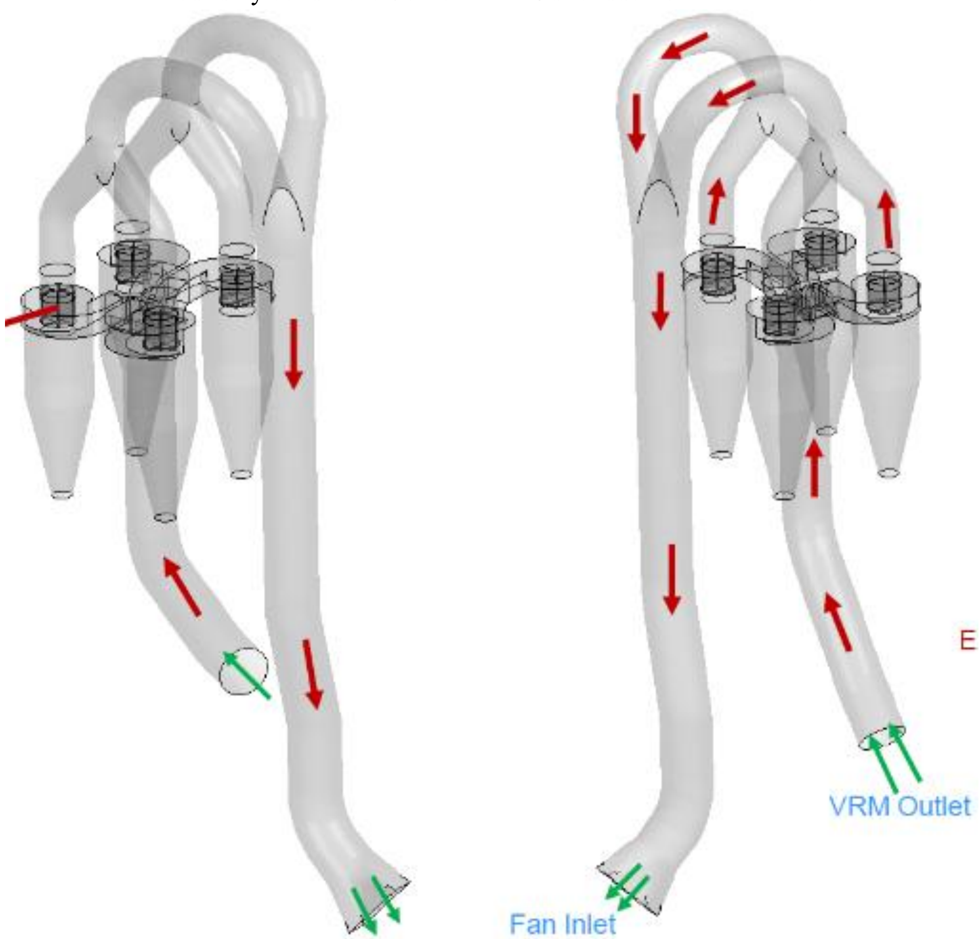

Figure 7. Inlet Conditions and its details for the study.

5. RESULTS AND DISCUSSIONS

The objective of the study is to optimize the flow pattern to get higher cyclone collection efficiency. The study is started with the analysis of Existing model flow analysis. Based on this study 3 different modifications in the Structure of the cyclone inlet are studied to get enhanced efficiency. The existing flow analysis is studied completely to see if there is any scope to improvise the flow with less structural changes. This study is first validated with initial analysis of existing model.

Validation of the results generated with the test data

Table 1. Measurement of Cyclone Efficiency of VRM(LM34.4).

Parameter	**UoM**	**Reading-1**	**Reading-2**	**Reading-3**
Flow at Cyclone Inlet,	m3/hr	440227	445105	451535
Dust at Cyclone Inlet, Cin	gm/m3	717	711	716
Dust at Cyclone Outlet, Cout	gm/m3	45.6	48.1	44.6
Cyclone efficiecy	%	93.6	93.2	93.8

An iso kinetic sampler (APM 620 of Envirotech Inst) used to measure mass of dust collected and volume of gas sampled.

Dust at Cyclone inlet, Cin = Mass of dust collected at Cyclone inlet/ Volume of gas sampled

Dust at Cyclone Outlet, Cout = Mass of dust collected at Cyclone outlet / Volume of gas sampled

Cyclone efficiency = (Cin- Cout)/Cin*100

The CFD showed cyclone efficiency 93.6 and the three sets of cyclone efficiencies are between 93.2 to 93.8, it means the CFD model is validated

The nature of flow through VRM Cyclone

The streamlines from inlet to the cyclone

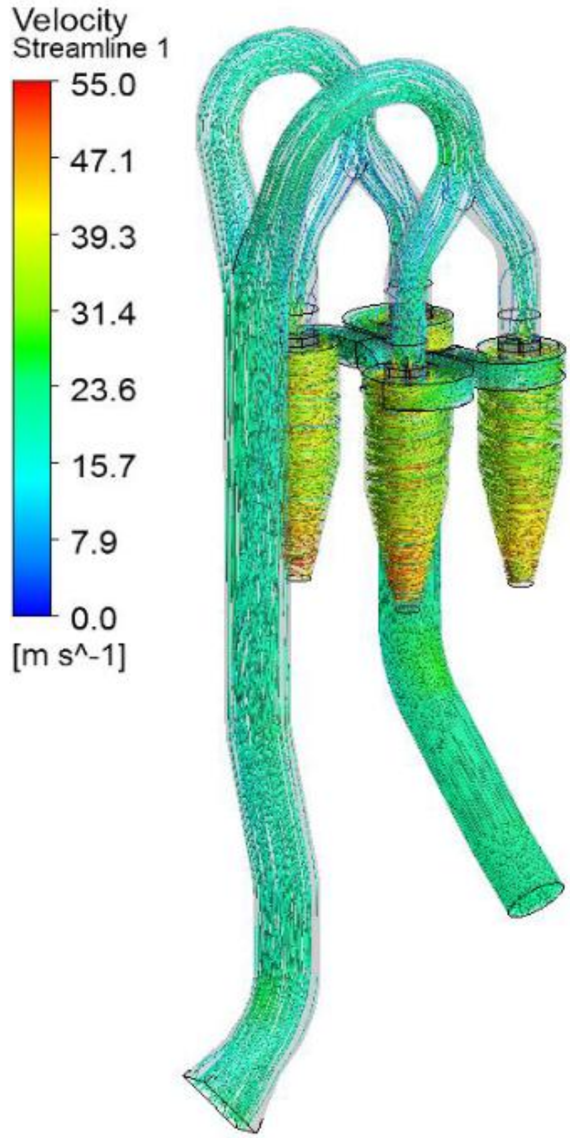

Figure 8. Streamlines from Inlet to the Fan outlet through VRM cyclone Existing.

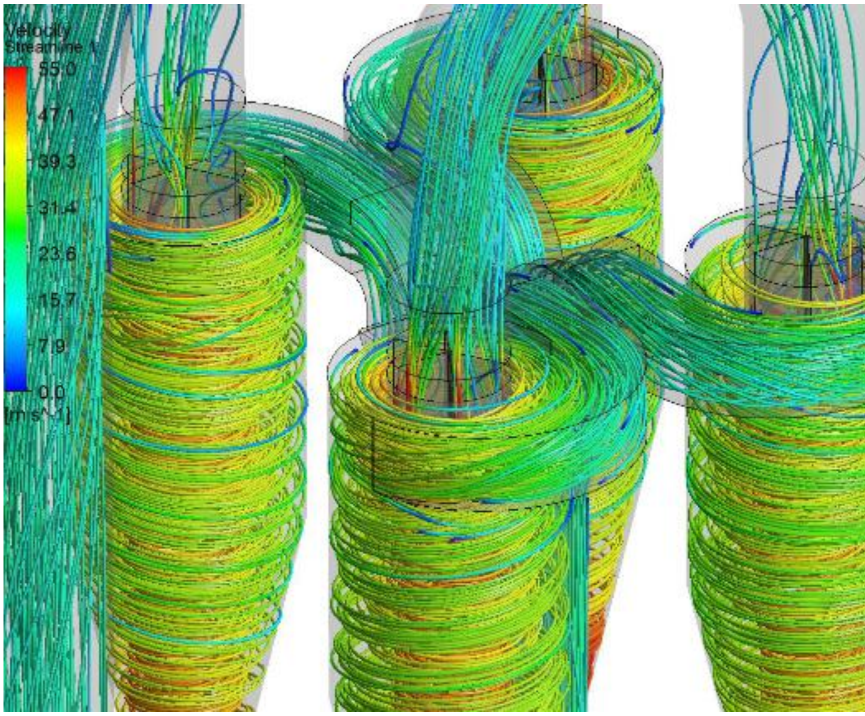

Figure 9. Streamlines through VRM cyclone Existing.

As can see the flow in the cyclone is uniform but at inlet of each Cyclone there is flow separation from the wall is observed and it can be seen from figure below that there is velocity stratification at each inlet of each cyclone so there is a scope of modification at this location. As a solution we are proposing that the guide plates are to be arranged at each inlet to improvise this flow. The provision of the guide plates can be seen in Fig. 15. These guide plates are curved, and their locations are as shown in the figure. These guide plates are fixed along the flow to modify the flow pattern.

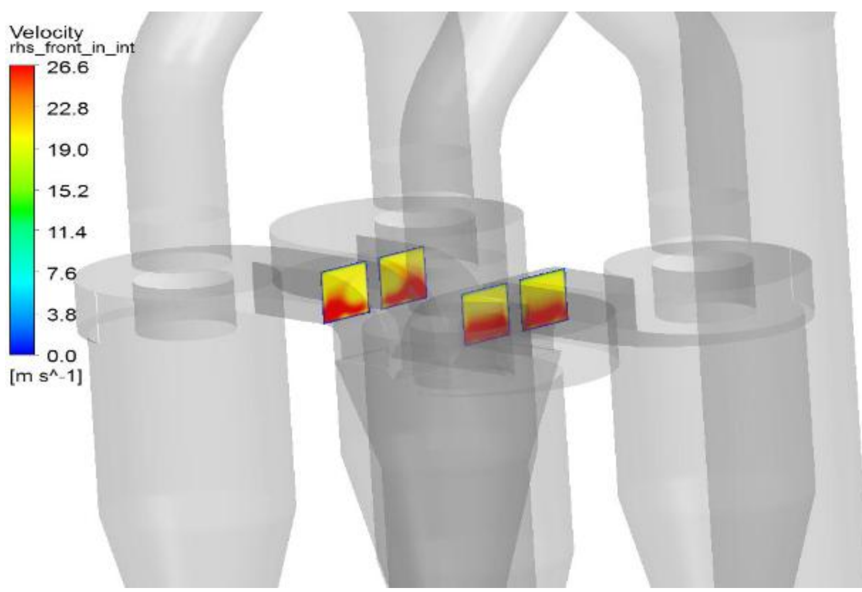

Figure 10. Contours at the inlet of VRM cyclone. Existing.

The figure 12 shows, velocity at inlet of cyclones is varying from 19 m/s to 26 m/s, the inlet of all cyclones are having velocity distribution like high velocity at bottom and low velocity at top, the velocity colour scale shows yellow colour for 19-20 m/s and red colour for 24 to 26 m/s for all cyclones. This high variation is the reason of high pressure drop

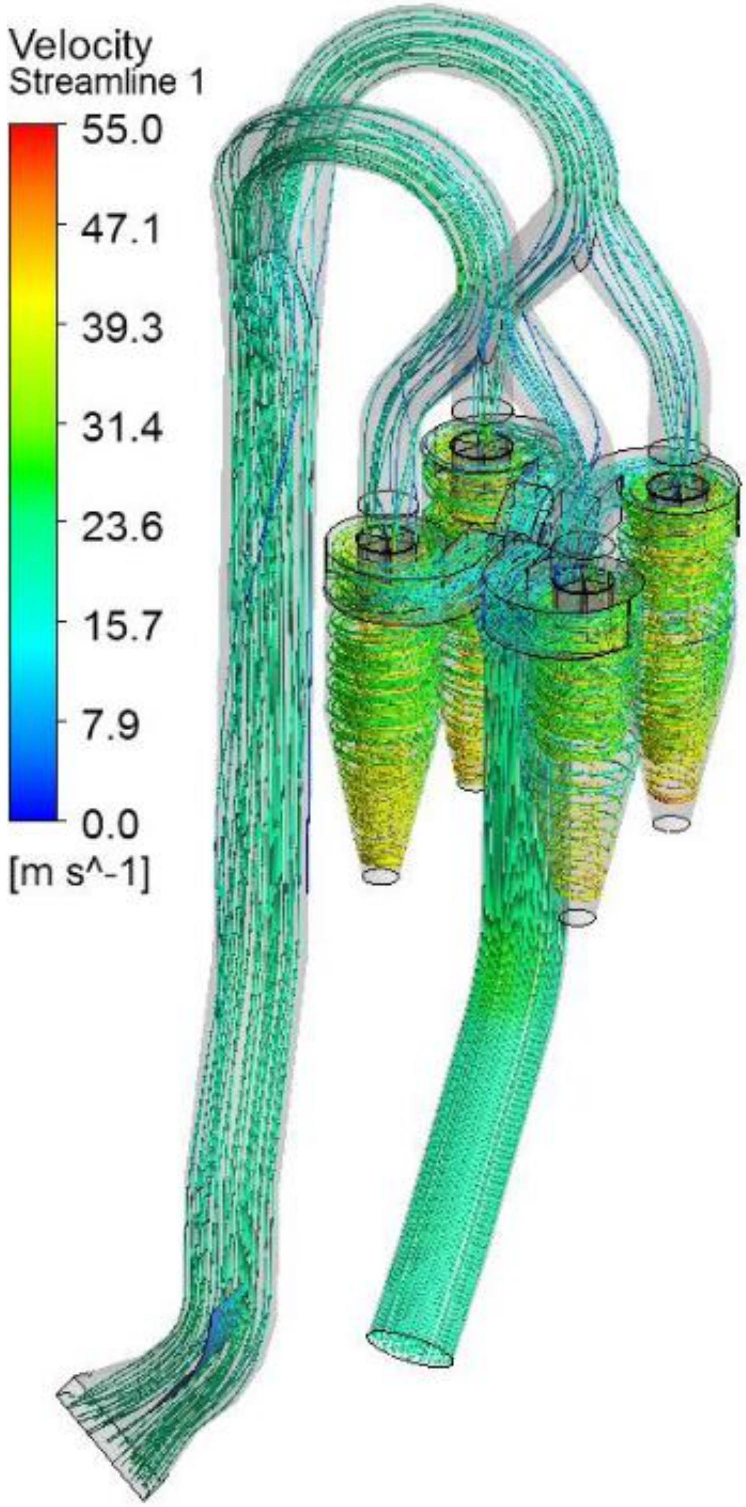

Figure 11. Streamlines from Inlet to the Fan outlet through VRM cyclone Modification.

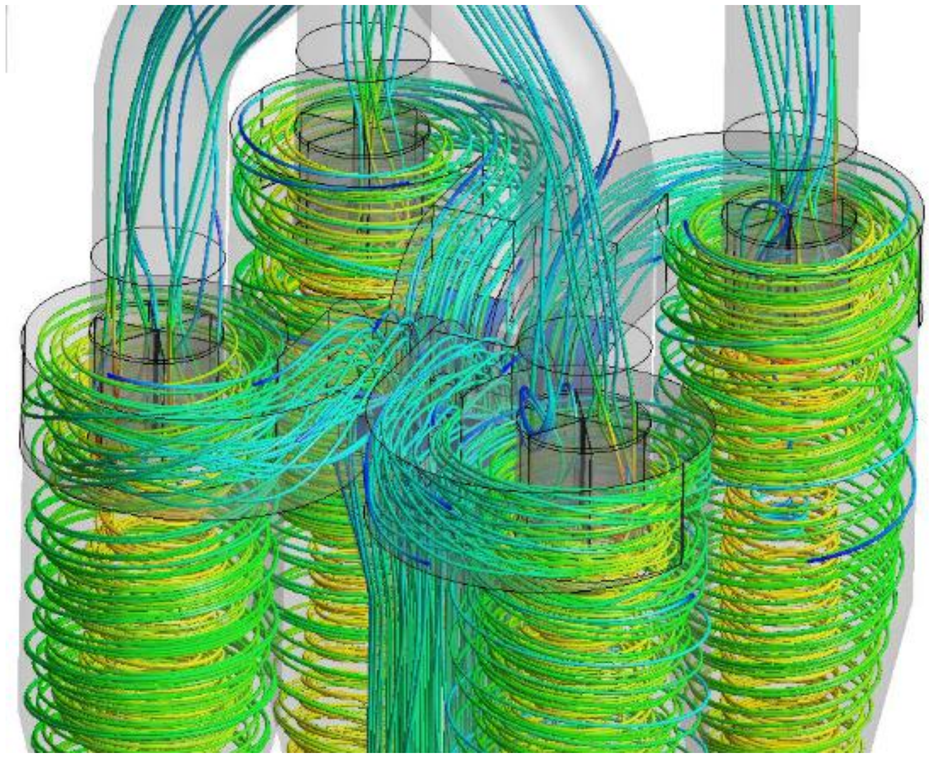

Figure 12. Streamlines through VRM cyclone Modification.

The provision of guide plates in a flow system significantly enhances flow characteristics by streamlining the fluid path, reducing recirculation zones, and improving flow uniformity. In CFD analysis, the following key improvements in the flow pattern can be observed: Reduction in Flow Separation & Recirculation Zones Without guide plates, the flow may separate at sharp bends or sudden expansions, leading to large-scale vortices and energy losses. Guide plates redirect the flow smoothly, minimizing separation and suppressing unwanted recirculation, resulting in a more attached and stable flow profile.

Improved Flow Distribution & Uniformity Guide plates help in evenly distributing the flow across the cross-section, preventing localized high-velocity or stagnant regions. CFD results typically show reduced velocity gradients and a more uniform velocity profile downstream of the guide plates. Pressure drop across bends or diffusers is significantly lowered due to reduced flow disturbances.

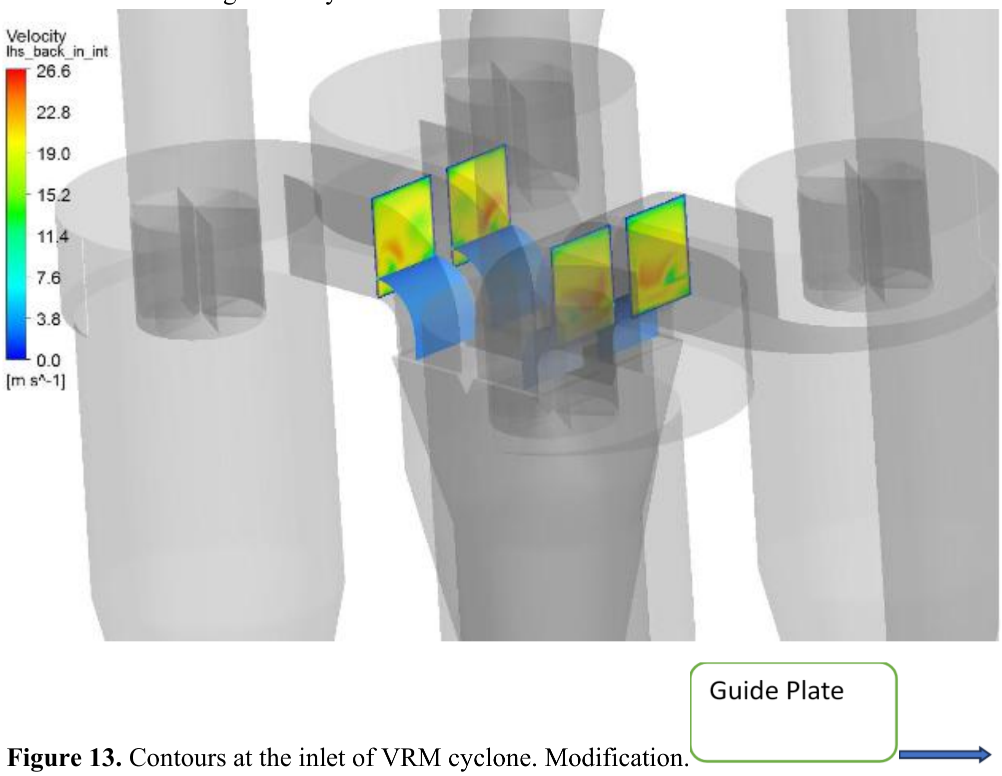

Figure 13. Contours at the inlet of VRM cyclone. Modification.

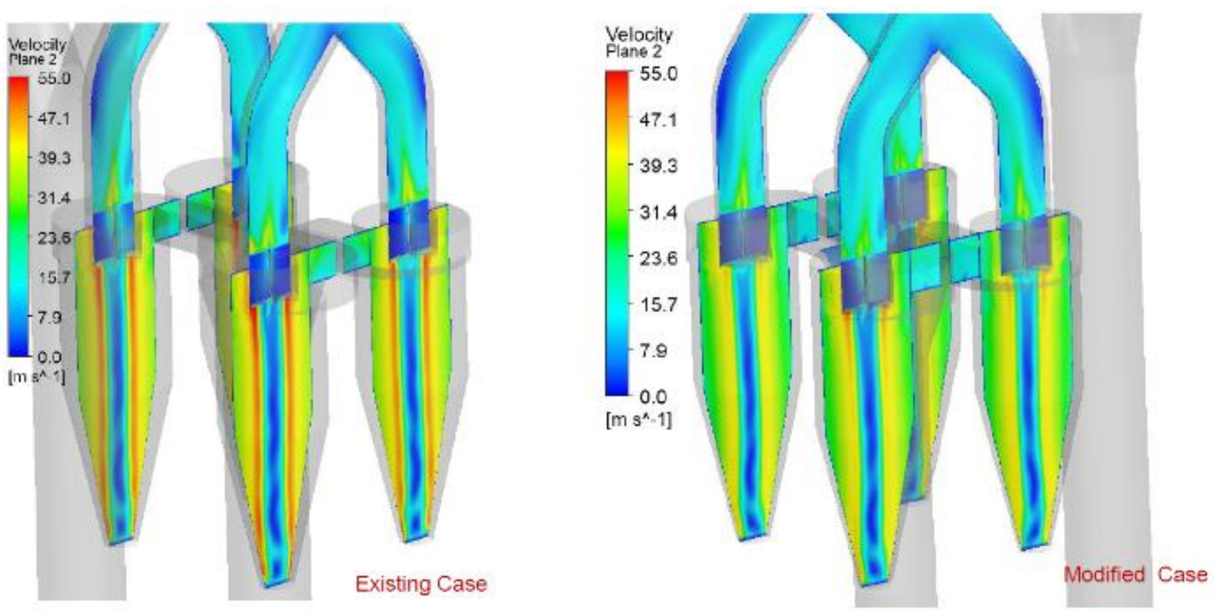

Figure 14. Contours at the inlet of VRM cyclone Comparative representation.

As we can see, the flow near the wall and at the core is improved from existing to modified case. This is achieved due to the provision of the guide vanes in the cyclone inlet duct. Velocity is also uniform across cyclone inlet, earlier it was varying between 19 to 26 m/s. After guide plate it is more uniform around 19 to 20 m/s.

In a duct or channel without guide plates, the flow often exhibits several undesirable characteristics:

Flow Separation & Recirculation Zones

1. At bends, expansions, or obstructions, the adverse pressure gradient causes flow separation, leading to large recirculation zones.
2. These vortices increase energy losses (pressure drop) and reduce system efficiency.
3. CFD Observation: Contour plots show low-velocity or reverse flow regions, while streamlines exhibit swirling patterns instead of smooth progression.

Non-Uniform Velocity Distribution

1. The flow tends to prefer one side of the duct, creating asymmetric velocity profiles.
2. This leads to hot spots, uneven heat transfer, or mechanical wear in industrial applications.
3. CFD Observation: Velocity magnitude contours show high-speed streaks near walls and stagnation zones in corners.

High Turbulence & Pressure Losses

1. Sharp turns or sudden area changes generate excessive turbulence, increasing turbulent kinetic energy (TKE), and dissipation.
2. Pressure drops are significantly higher due to flow disturbances and momentum loss.
3. CFD Observation: High TKE regions near bends and elevated total pressure loss in post-processing.

Secondary Flows & Swirl Effects

1. In curved ducts, Dean vortices or crossflow circulations develop, distorting the primary flow direction.
2. These secondary flows reduce effective flow area and degrade performance.
3. CFD Observation: Vector plots show transverse velocity components disrupting axial flow.

Flow Improvement with Guide Plates

The introduction of guide plates systematically addresses these issues, leading to a more efficient, stable, and uniform flow.

Elimination of Flow Separation & Recirculation

Guide plates gradually redirect the flow, preventing sudden flow detachment.

CFD Observation

1. Streamlines remain attached to the duct walls without reverse flow.
2. Recirculation zones shrink or disappear entirely in contour plots.

Uniform Velocity Distribution

Guide plates split and guide the flow evenly, avoiding preferential pathways.

CFD Observation

1. Velocity contours show symmetrical distribution with no dead zones.
2. Reduced velocity gradients, ensuring balanced flow in heat exchangers or reactors.

Reduced Turbulence & Pressure Drop

The smoothened flow path minimizes turbulent eddies and energy dissipation.

CFD Observation

1. Lower TKE values near guide plates compared to unguided cases.
2. Reduced total pressure loss (up to 30-50% in optimized designs).

Suppression of Secondary Flows

Guide plates break down Dean vortices and realign the flow axially.

CFD Observation

1. Vector plots show dominant axial flow with minimal transverse components.
2. Path lines remain straight, improving mass/heat transfer efficiency.

Table 2. CFD Validation Metrics for Performance Comparison.

Parameter	**Without Guide Plates**	**With Guide Plates**
Recirculation Zones	Large, persistent vortices	Minimal or eliminated
Pressure Drop (ΔP)	High due to separation losses	Significantly lower
Flow Uniformity	Asymmetric, high gradients	Balanced velocity distribution

The strategic placement of guide plates transforms chaotic, inefficient flow into a streamlined, low-loss, and uniform motion, as clearly evidenced by CFD simulations. This technique outperforms alternative passive flow control methods by combining simplicity, effectiveness, and adaptability, making it a preferred solution for industrial and aerodynamic applications.

The Flow in the Cyclone

Flow Distribution plays important role in pressure drop in Existing model the Cyclone. This causes uneven distribution of flow in cross sectional area at the inlet of each cyclone. This leads to the adverse effect on pressure drop [28–30]. At core, there is also a non-uniform average velocity distribution that can be observed which will ultimately cause maximum pressure drop. It observed that there are multiple parameters are there which governs the change in pressure drop. From experience we have used height that needs to be changed from its original size. The modification starts from changing the flow area by changing cyclone inlet height 1197 mm. This modification is done in –ve Z-direction and in +ve Z-direction. In modification, the flow area is increased by changing the height. With change in height from 1197 to 1497 in –Z direction, the obtained results show that at 1497 mm height the pressure drop reduced to 148 mmWC from 198 mmWC and this shows that the velocity distribution is uniform and is consistent throughout the cyclone. This will result in reduction in average velocity at core and ultimately reduced the Pressure drop.

Originally the height of cyclone was 1197 mm, and weight was also 1197 mm means and area is 1.43m2

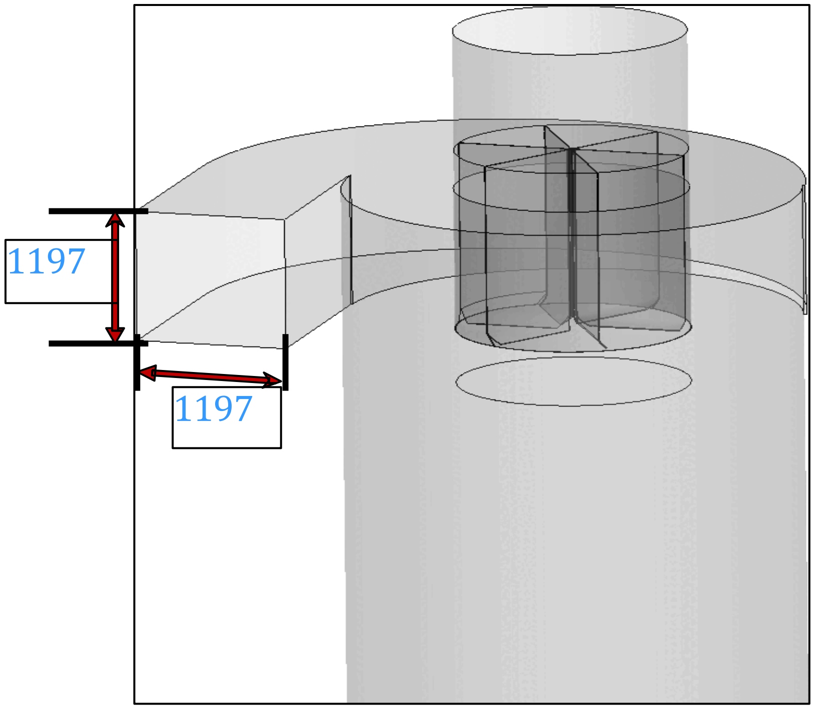

Figure 15. Original Cyclone inlet dimensions.

Modification 01

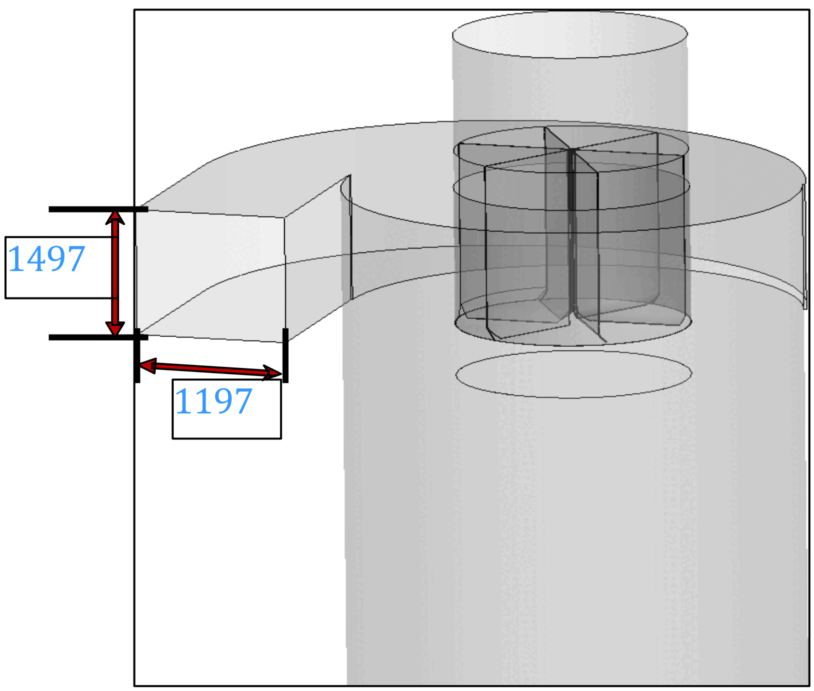

Figure 16. Modified Cyclone inlet dimensions.

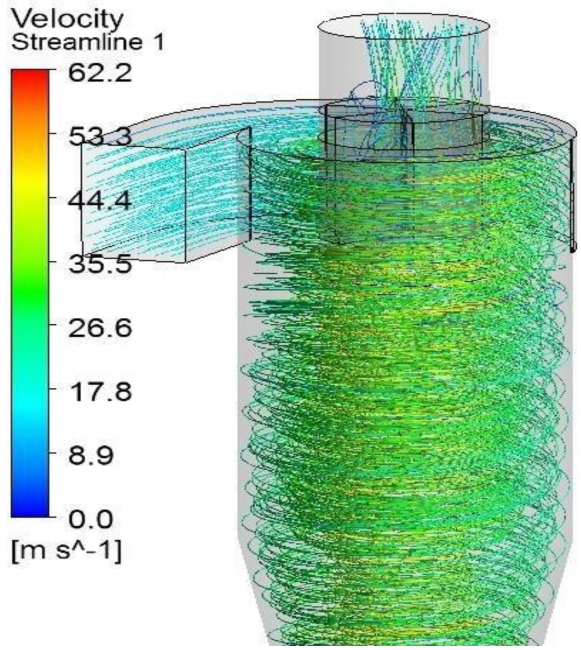

Figure 17. CFD of Modified as per Modification 1.

In this Case Inlet height is increased by 300 mm from existing height 1197 mm and area is 1.791 m2, width to height ration is 0.8 and flow distribution is more improved as compared to existing where with to height ratio is 1.

Modification 02

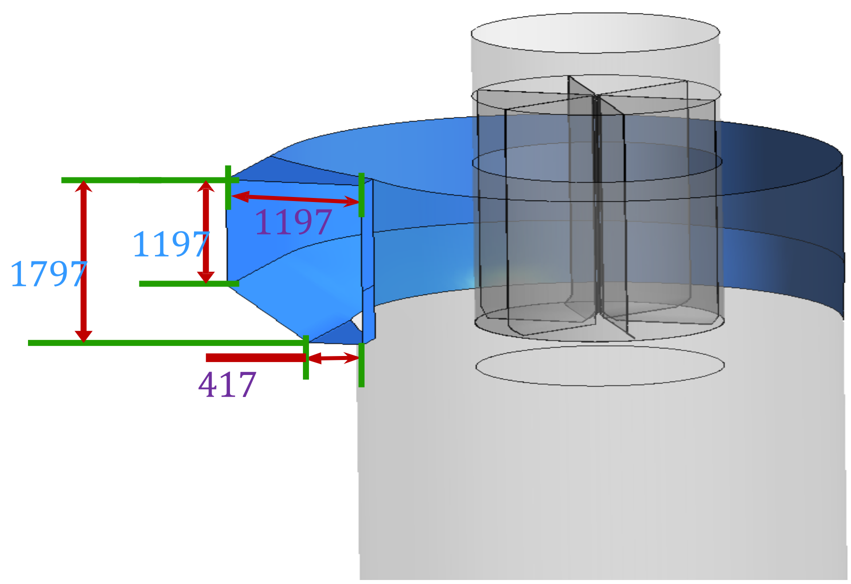

Figure 18. Modified Cyclone inlet Shape.

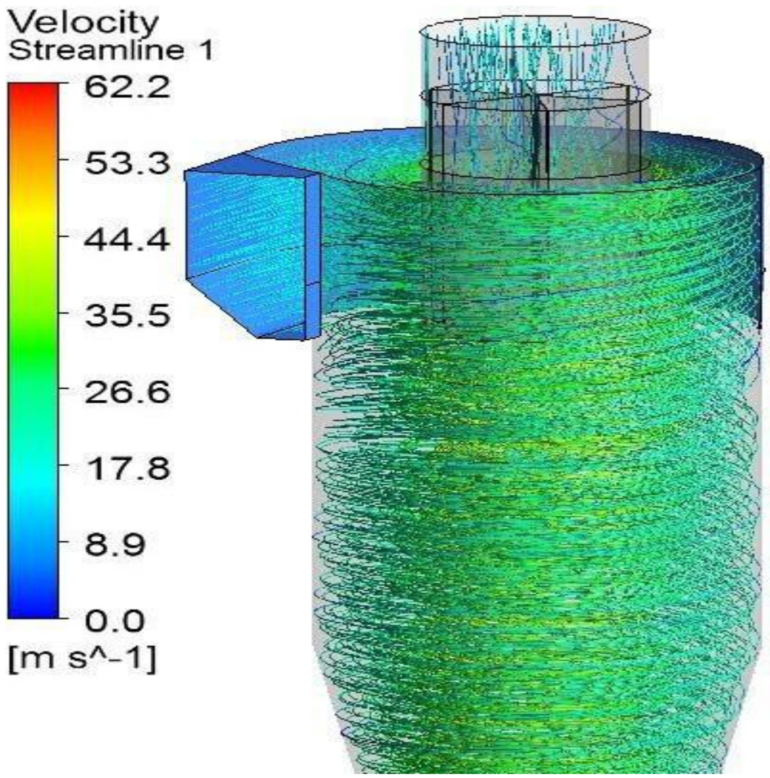

Figure 19. CFD of Modified as per Modification 2.

Inlet Area Changed to 1.659 m2 by modifying the cyclone inlet in pentagon shape. Inlet Height is 1.767 m2 by modifying cylindrical height, flow distribution is improved and even better than modification 1

Modification 03

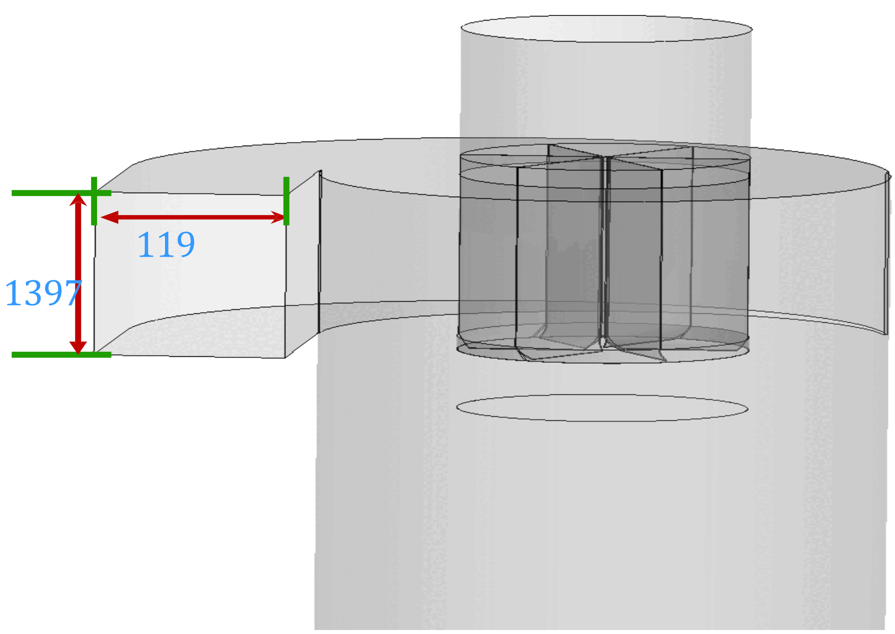

Figure 20. Modified inlet shape for modification 3.

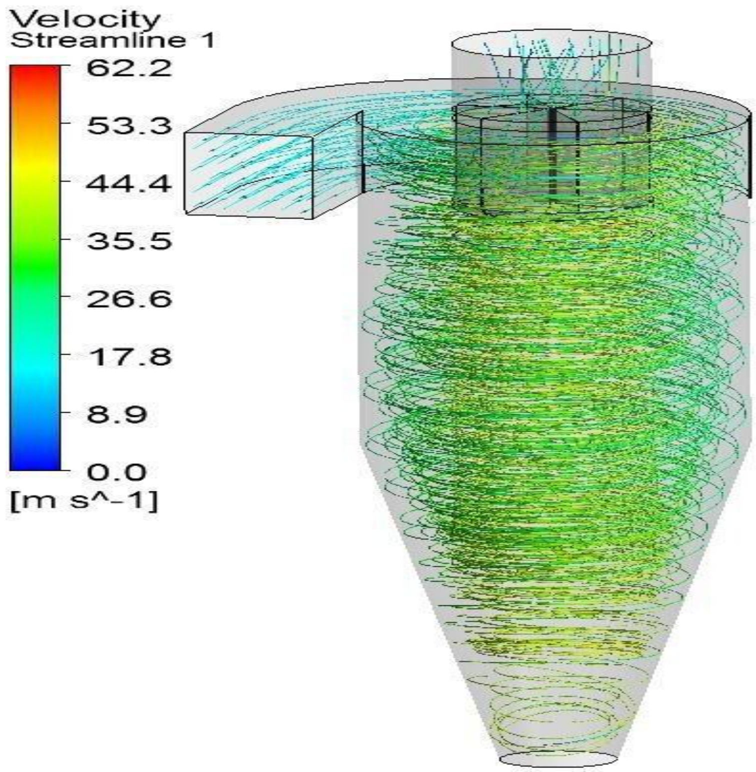

Figure 21. CFD of Modified as per Modification 3.

In this Case Inlet height is increased by 200 mm from existing height 1197 mm and area is 1.672 m2, width to height ration is 0.856 and flow distribution is more improved as compared to existing where with to height ratio is 1.

Table 3. Result Pressure Drop and Efficiency details.

Case	**Pressure drop**	**Overall Collection efficiency**
Existing	198 MMWC	93.60%
Modification 01	148 MMWC	91.54%
Modification 02	131 MMWC	90.39%
Modification 03	162 MMWC	92.46%

The presented cases evaluate dimensional modifications to an existing flow system (likely a dust collector, cyclone separator, or electrostatic precipitator) with the following objectives:

1. Reduce pressure drop (ΔP) to minimize energy consumption.
2. Maintain high collection efficiency to ensure effective particulate separation.

The trade-off between these two parameters is critical—excessive pressure drop increases operational costs, while poor collection efficiency leads to compliance risks and environmental concerns.

Performance Evaluation of Modifications

Baseline (Existing System)

Pressure Drop: 198 MMWC (high energy consumption)

Collection Efficiency: 93.60% (excellent capture rate)

Key Issue: The high ΔP suggests excessive flow resistance, likely due to:

1. Sharp bends or contractions
2. Poorly optimized internal baffles/vanes
3. Inefficient inlet/outlet design

Modification 01 (Optimal Design)

Pressure Drop: 148 MMWC (↓20.2%)

Collection Efficiency: 91.54% (↓2.06%)

Advantages

1. Significant ΔP reduction (~40 MMWC savings) → Lower fan power, reduced operating costs.
2. Minimal efficiency loss (still above 91%) → Regulatory compliance maintained.
3. Likely improvements:
4. Smoother flow path (reduced turbulence)
5. Optimized guide vanes or diffuser angles
6. Better flow distribution across filters/collectors

Modification 02 (Over-Optimized for ΔP)

1. Pressure Drop: 131 MMWC (↓33.8%)
2. Collection Efficiency: 90.39% (↓3.21%)
3. Drawbacks:
4. Efficiency drop is too steep → Potential non-compliance in strict emission standards.
5. Likely causes:
6. Excessive flow straightening (reducing particle settling time)
7. Reduced swirl effects (critical for centrifugal separators)
8. Wider flow passages (lowering particle impaction probability)

Modification 03 (Suboptimal Trade-Off)

1. Pressure Drop: 162 MMWC (↓23.2%)
2. Collection Efficiency: 92.46% (↓1.14%)
3. Analysis:
4. Better efficiency than Mod 01, but ΔP reduction is less significant (only 36 MMWC vs. 50 MMWC).
5. Not cost-effective—Mod 01 achieves nearly the same ΔP savings with only a slightly lower efficiency.

Optimal Balance Between Energy Savings & Performance

1. ΔP Reduction (20.2%) → Direct energy savings (fan power ∝ ΔP).
2. Efficiency Drop (2.06%) → Negligible impact on emission control.

Economic Justification

1. Lower operational costs due to reduced ΔP.

2. No need for additional retrofitting (unlike Mod 02, which may require supplemental filtration).
3. Likely involves minor geometric adjustments (e.g., guide vane angle optimization) rather than major redesigns.
4. Easier to implement compared to more aggressive modifications (Mod 02).

Table 4. Performance Comparison of Modifications.

Case	Pressure Drop (MMWC)	Overall Collection Efficiency (%)	Key Observations
Existing	198	93.60%	Baseline (high ΔP, best efficiency)
Modification 01	**148**	**91.54%**	**Optimal balance** (significant ΔP reduction, minor efficiency drop)
Modification 02	131	90.39%	Lowest ΔP but **excessive efficiency loss**
Modification 03	162	92.46%	Better efficiency than Mod 01 but **higher ΔP**

Modification 01: The Optimal Solution

1. Pressure Drop Reduction: ~20.2% decrease (198 → 148 MMWC) – A substantial improvement, leading to lower fan power consumption.
2. Efficiency Impact: Only ~2.06% drop (93.6% → 91.54%) – A minor sacrifice for significant energy savings.
3. Why It's the Best?
4. Achieves the best trade-off between ΔP reduction and efficiency retention.
5. Further ΔP reductions (Mod 02) come at too high an efficiency cost.
6. Mod 03 improves efficiency slightly but does not justify the higher ΔP compared to Mod 01.

Modification 02: Excessive Focus on Pressure Drop

1. Lowest ΔP (131 MMWC, ~33.8% reduction) but efficiency drops to 90.39% (3.21% loss).
2. Unacceptable for most industrial applications where collection efficiency is critical.

Modification 03: Slightly Better Efficiency but Inferior ΔP

1. Higher ΔP (162 vs. 158 MMWC in Mod 01) with only ~0.92% efficiency gain (92.46% vs. 91.54%).
2. Not justified, as Mod 01 already provides near-optimal efficiency with better ΔP savings.

Table 5. VRM Comparison After Cyclone Modification.

S.No	Parameter	Unit	Before study	After Modification	▲P
1	VRM Feed	TPH	325	335	
2	RM Fan speed	rpm	868	844	
3	RM fan power	Kw	1795	1710	

Pressure Profile					
4	Mill Inlet	mmWG	-80	-78	-2
5	Mill Outlet	mmWG	-890	-880	-10
6	Common duct	mmWG	-905	-902	-3
7	CY-1 Inlet	mmWG	-974	-945	-29
8	CY-1 Outlet	mmWG	-1080	-1020	-60
9	DP Across Cyclone-1	mmWG	106	75	31
10	CY-2 Inlet	mmWG	-974	-956	-18
11	CY-2 Outlet	mmWG	-1085	-1025	-60
12	DP Across Cyclone-2	mmWG	111	69	42
13	CY-3 Inlet	mmWG	-942	-955	13
14	CY-3 Outlet	mmWG	-1065	-1040	-25
15	DP Across Cyclone-3	mmWG	123	85	38
16	CY-4 Inlet	mmWG	-970	-960	-10
17	CY-4 Outlet	mmWG	-1085	-1038	-47
18	DP Across Cyclone-4	mmWG	115	78	37
19	Transverse point	mmWG	-1100	-1050	-50
20	RM Fan Inlet	mmWG	-1115	-1065	-50
21	RM Fan Outlet	mmWG	-58	-54	-4
22	RM Fan Flow	m^3/hr	464136	464472	

6. CONCLUSION

This study is based on the two perspectives first is to reduce the pressure drop and second is to increase the Overall collection efficiency.

The study carried out considers two distinct locations where the flow needs to be optimized. The first location is the Duct from ID Fan to Cyclone; second is the shape of inlet duct to cyclone.

In the first location where the Flow from ID fan about to enter the Cyclone is optimized by providing the Guide Plates. Before provision of the Guide Plates, the flow is non uniform, and there is stratification in the Flow Velocity. The modification by providing the Guide Plates caused the flow to be uniform in such a way that there are less flow reversal and reduction in flow stratification.

In the second location, i.e. the Inlet area of the cyclone is changed to optimize the flow pattern in order to increase the overall collection efficiency. The Area and shape of the inlet of Cyclone is configured into three modifications in such way that shape and area is different.

Out of proposed modifications, the modification 02 and 03 found observations as like, with modification 02 the pressure drop is 131 mmWC and overall collection efficiency of 90.39% and modification 03 the pressure drop is 162 mmWC and overall collection efficiency of 92.46%.

The Pressure drop is the function of flow velocity and flow uniformity, and this is vital parameter in the assessment of performance analysis of Plant. On the other hand, the overall collection efficiency is the function of the flow pattern and its velocity and core generation in the cyclone so that the size-wise separation of the particle can be achieved.

In this study, it is evident that modification 02 can be applicable on account of the sacrifice of 1% overall collection efficiency which is less than modification 03 but the pressure drop in modification 03 is of 162 mmWC.

At a modified height of 300mm, flow is uniform, and this results in a reduction in velocity distribution. This results in a reduction of pressure drop by 50 mmWG. With a compromise of 1% in collection efficiency, the system saving is of 85 units/hr.

The study is carried out using CFD tool, based on the results obtained during study, it is concluded that computational fluid dynamics is the best tool to assess the performance of the system in an economic way. This reduces pressure drop across cyclone. Considering the economic perspective, it is evident that the Power Saving achieved with new proposed modifications is - 85 units/hr (617100 units/Annum), In expenses it is observed Total monetary saving of Rs. 33.94 lakhs/Annum.

This also reduced the CO_2 Generation by 506022 Kg CO_2/Annum. As per the proposed modifications, the investigation reveals that the implementation of these modifications will cost approximately Rs. 11 Lakh.

REFERENCES

1. E. Dehdarinejad, M. Bayareh, Analysis of the vortical flow in a cyclone using four vortex identification methods, Powder Technol. 428 (2023) 118897. https://doi.org/10.1016/j.powtec.2023.118897.
2. T.V. Paganel, E.F. Alban, M.A. Cyrille, C.V.N. Abbe, CFD Simulation of an Industrial Dust Cyclone Separator: A Comparison with Empirical Models: The Influence of the Inlet Velocity and the Particle Size on Performance Factors in Situation of High Concentration of Particles, Journal of Engineering 2024 (2024) 5590437. https://doi.org/10.1155/2024/5590437.
3. J. Wei, H. Zhang, Y. Wang, Z. Wen, B. Yao, J. Dong, The gas-solid flow characteristics of cyclones, Powder Technol. 308 (2017) 178–192. https://doi.org/10.1016/j.powtec.2016.11.044.
4. A. Raoufi, M. Shams, M. Farzaneh, R. Ebrahimi, Numerical simulation and optimization of fluid flow in cyclone vortex finder, Chemical Engineering and Processing: Process Intensification 47 (2008) 128–137. https://doi.org/10.1016/J.CEP.2007.08.004.
5. K. Elsayed, C. Lacor, CFD modeling and multi-objective optimization of cyclone geometry using desirability function, Artificial neural networks and genetic algorithms, Appl. Math. Model. 37 (2013) 5680–5704. https://doi.org/10.1016/j.apm.2012.11.010.
6. A.J. Hoekstra, J.J. Derksen, H.E.A. Van Den Akker, An experimental and numerical study of turbulent swirling flow in gas cyclones, Chem. Eng. Sci. 54 (1999) 2055–2065. https://doi.org/10.1016/S0009-2509(98)00373-X.
7. A.A. Vegini, H.F. Meier, J.J. Less, M. Mori, Computational fluid dynamics (CFD) Analysis of cyclone separators connected in series, Ind. Eng. Chem. Res. 47 (2008) 192–200. https://doi.org/10.1021/IE061501H.
8. C. Mingham, L. Qian, D. Causon, Computational Fluid Dynamics (CFD) Models, Numerical Modelling of Wave Energy Converters: State-of-the-Art Techniques for Single Devices and Arrays (2016) 105–122. https://doi.org/10.1016/B978-0-12-803210-7.00006-2.
9. W.D. Griffiths, F. Boysan, Computational fluid dynamics (CFD) and empirical modelling of the performance of a number of cyclone samplers, J. Aerosol Sci. 27 (1996) 281–304. https://doi.org/10.1016/0021-8502(95)00549-8.
10. P. Katare, A. Krupan, A. Dewasthale, A. Datar, A.S. Dalkilic, CFD analysis of cyclone separator used for fine filtration in separation industry, Case Studies in Thermal Engineering 28 (2021) 101384. https://doi.org/10.1016/J.CSITE.2021.101384.
11. K.W. Chu, B. Wang, D.L. Xu, Y.X. Chen, A.B. Yu, CFD–DEM simulation of the gas–solid flow in a cyclone separator, Chem. Eng. Sci. 66 (2011) 834–847. https://doi.org/10.1016/J.CES.2010.11.026.
12. M. Mirzaei, S. Clausen, H. Wu, S. Zakrzewski, M. Nakhaei, H. Zhou, K. Martin Jønck, P. Arendt Jensen, W. Lin, CFD simulation and experimental validation of multiphase flow in industrial cyclone preheaters, Chemical Engineering Journal 465 (2023) 142757. https://doi.org/10.1016/J.CEJ.2023.142757.
13. K. Elsayed Khairy, C. Lacor, Optimization of the cyclone separator geometry for minimum pressure drop using mathematical models and CFD simulations, Chem. Eng. Sci. 65 (2010) 6048–6058. https://doi.org/10.1016/J.CES.2010.08.042.
14. K. Chu, Y. Chen, L. Ji, Z. Zhou, A. Yu, J. Chen, Coarse-grained CFD-DEM study of Gas-solid flow in gas cyclone, Chem. Eng. Sci. 260 (2022) 117906. https://doi.org/10.1016/j.ces.2022.117906.

15. R.D. Luciano, B.L. Silva, L.M. Rosa, H.F. Meier, Multi - objective optimization of cyclone separators in series based on computational fluid dynamics, Powder Technol. 325 (2018) 452–466. https://doi.org/10.1016/J.POWTEC.2017.11.043.
16. Y. Huang, M.Q. Zhao, H.T. Liu, Numerical Simulation of the Gas Phase of Cyclone-Separator Sand Trap Based on ICEM CFD and FLUENT, Adv. Mat. Res. 774–776 (2013) 321–325. https://doi.org/10.4028/www.scientific.net/AMR.774-776.321.
17. C. Cortés, A. Gil, Modeling the gas and particle flow inside cyclone separators, Prog. Energy Combust. Sci. 33 (2007) 409–452. https://doi.org/10.1016/J.PECS.2007.02.001.
18. Z.W. Zhang, Q. Li, Y.H. Zhang, H.L. Wang, Simulation and experimental study of effect of vortex finder structural parameters on cyclone separator performance, Sep. Purif. Technol. 286 (2022) 120394. https://doi.org/10.1016/J.SEPPUR.2021.120394.
19. A. Avci, I. Karagoz, Effects of flow and geometrical parameters on the collection efficiency in cyclone separators, J. Aerosol Sci. 34 (2003) 937–955. https://doi.org/10.1016/S0021-8502(03)00054-5.
20. D.K. Le, J.Y. Yoon, A hybrid CFD – Deep learning methodology for improving the accuracy of pressure drop prediction in cyclone separators, Chemical Engineering Research and Design 190 (2023) 296–311. https://doi.org/10.1016/J.CHERD.2022.12.035.
21. E. Bernardini, S.M.J. Spence, D. Wei, A. Kareem, Aerodynamic shape optimization of civil structures: A CFD-enabled Kriging-based approach, Journal of Wind Engineering and Industrial Aerodynamics 144 (2015) 154–164. https://doi.org/10.1016/J.JWEIA.2015.03.011.
22. Q. Li, C. Ye, Y. Jia, Numerical Simulation Study on Separation Performance of Cyclone Separator Based on Fluent, International Core Journal of Engineering 7 (n.d.) 2021. https://doi.org/10.6919/ICJE.202112_7(12).0040.
23. D. Cokljat, M. Slack, S.A. Vasquez, A. Bakker, G. Montante, Reynolds-stress model for Eulerian multiphase, Progress in Computational Fluid Dynamics 6 (2006) 168–178. https://doi.org/10.1504/PCFD.2006.009494.
24. I. Ben Hassan Saïdi, M. Schmelzer, P. Cinnella, F. Grasso, CFD-driven symbolic identification of algebraic Reynolds-stress models, J. Comput. Phys. 457 (2022) 111037. https://doi.org/10.1016/j.jcp.2022.111037.
25. A.M. Jawarneh, G.H. Vatistas, Reynolds Stress Model in the Prediction of Confined Turbulent Swirling Flows, J. Fluids Eng. 128 (2006) 1377–1382. https://doi.org/10.1115/1.2354530.
26. C.H. Park, S.O. Park, A compressible turbulence model for the pressure-strain correlation, Journal of Turbulence 6 (2005). https://doi.org/10.1080/14685240500055095.
27. J. Selvanayagam, C. Aliaga, J. Stokes, CFD simulation of S-duct test case using ANSYS FLUENT, AIAA Propulsion and Energy Forum and Exposition, 2019 (2019). https://doi.org/10.2514/6.2019-3847.
28. H. Feldman, D. Leith, Cyclone optimization based on a new empirical model for pressure drop, Aerosol Science and Technology 15 (1991) 135–148. https://doi.org/10.1080/02786829108959520.
29. B. Blocken, Computational Fluid Dynamics for urban physics: Importance, scales, possibilities, limitations and ten tips and tricks towards accurate and reliable simulations, Build. Environ. 91 (2015) 219–245. https://doi.org/10.1016/j.buildenv.2015.02.015.
30. Y. Tominaga, L. (Leon) Wang, Z. (John) Zhai, T. Stathopoulos, Accuracy of CFD simulations in urban aerodynamics and microclimate: Progress and challenges, Build. Environ. 243 (2023) 110723. https://doi.org/10.1016/J.BUILDENV.2023.110723.